Mon. Not. R. astr. Soc. (1987) **226,** 493–504

The dynamics of the giant ring nebula Hubble III in NGC 6822

C. A. Clayton *Department of Astronomy, The University, Manchester M13 9PL*

Accepted 1987 January 5. Received 1986 December 15; in original form 1986 November 24

Summary. The dynamics and the structure of the ring nebula Hubble III in NGC 6822 have been investigated by obtaining absolutely calibrated Hα imagery of the object and Hα line profiles along two orthogonal lines across its face using the Manchester Echelle Spectrometer II.

A remarkably symmetric radially expanding bubble is observed with smaller expanding bubbles over its surface. Several possible dynamical origins are examined and models involving stellar wind driven bubbles are found to be the most convincing.

The kinematics of the neighbouring nebula Hubble I are also briefly discussed.

1 Introduction

The irregular galaxy NGC 6822 in our local group contains many H II regions, the brightest of which were first catalogued by Hubble (1925). One of these nebulae, Hubble III (also known as Hodge 4, NGC 6822B and NGC 6822-2) appears as a complete ring of nebulosity, some 50 arcsec in diameter, surrounding a cluster of bright stars. Its appearance is very similar to the filamentary nebulae found in the LMC (see Meaburn 1981 for a summary and references therein), in particular the circular ring-like nebula N70. The origin of these objects has been the subject of some debate. Morphologically similar nebulae often appear to have quite diverse dynamical natures and in some specific cases (for example, N70), no model has yet been generally accepted.

In this paper the dynamics and morphology of Hubble III are investigated in an attempt to determine the origin of this highly symmetric object and to allow a comparison with other structurally similar nebulae to be made. This has been achieved by obtaining Hα line profiles across this object and Hα imagery of the nebulosity.

2 Observations and results

The observations described below were obtained using the dedicated Manchester Echelle Spectrometer II (Meaburn *et al.* 1984). The instrument was used at the $f/15$ Cassegrain focus of the 2.5-m Isaac Newton Telescope on La Palma in conjunction with the two-dimensional photon-counting detector, IPCS (Boksenberg & Burgess 1973). All data reduction was achieved using software available on the Manchester node of the STARLINK network.

2.1 Imagery

The Hα image of Hubble III and the neighbouring Hubble I illustrated in Plate 1 was obtained using the Manchester Echelle in its direct imaging mode through a 90 Å bandwidth interference filter centred on Hα and [N II]. The integration time was 1254 s. NGC 6822 is underabundant in nitrogen by a factor of 6 compared with our own Galaxy (Peimbert & Spinrad 1970) and thus 95 per cent of the emission passed is Hα. This figure is derived from the Hα and [N II] ratios obtained from the spectra discussed in Section 2.2. The image has been filtered to reduce noise in relatively flat areas whilst still preserving sharp edges. This was achieved using local statistics to locate steep gradients in the data (Lee 1981). Some minor distortion has been introduced by the IPCS. The image is orientated such that increasing increments for position 1 run from right to left and for position 2 from bottom to top (see Fig. 1).

The image has been calibrated in absolute Hα intensity against the standard star BD+28°4211. A value of 6.6×10^{-12} erg cm^{-2} s^{-1} was obtained for the total Hα intensity of the Hubble III nebulosity after correcting for reddening (Seaton 1979; Hodge 1977) and [N II] contamination.

For comparison, the best available continuum photograph of Hubble III can be found in Malin & Murdin (1984) which also shows the whole of NGC 6822 and the other bright emission nebulae.

2.2 LINE PROFILES

The line profiles were obtained from an entrance slit 141 arcsec long and 300 μm wide ($\equiv$20 km s^{-1}). This is equivalent to 1.65 arcsec when projected on the sky by the INT. Two hundred and forty data taking windows (each 0.59 arcsec long) were placed along the slit and 1020 in the direction of dispersion. A 90 Å bandwidth interference filter was used to isolate a single échelle order containing the Hα and [N II] emission.

The location of both slit positions over the face of the nebula are shown against a sketch of the stars and nebulosity in Fig. 1. The position angles of the slits were chosen so as to be orthogonal and such that one of the slit positions would cover the adjacent H II region, Hubble I, in order to examine the kinematics there. These are briefly discussed in Section 3.4. The integration time for

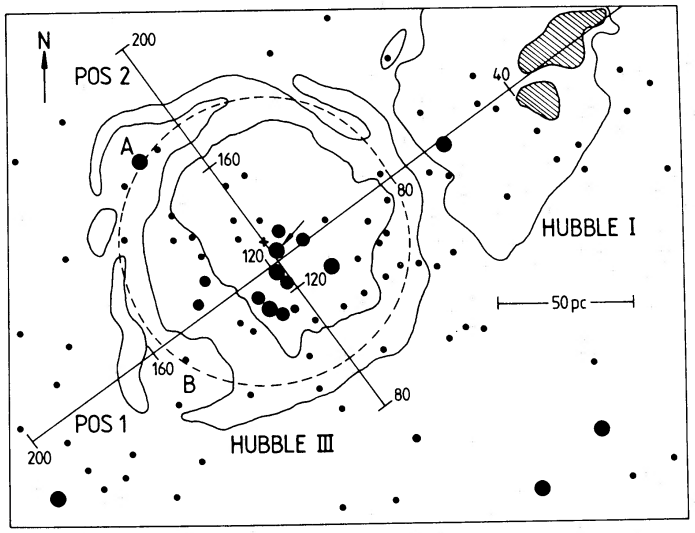

Figure 1. A schematic diagram of Hubble III and I showing the location of the two slit positions, with slit increments marked. The small cross close to the central stars marks the centre of the dotted circle. The star F9 mentioned in the text is indicated by the arrow and the shaded area in Hubble I shows the position of a concentration of bright gas and stars.

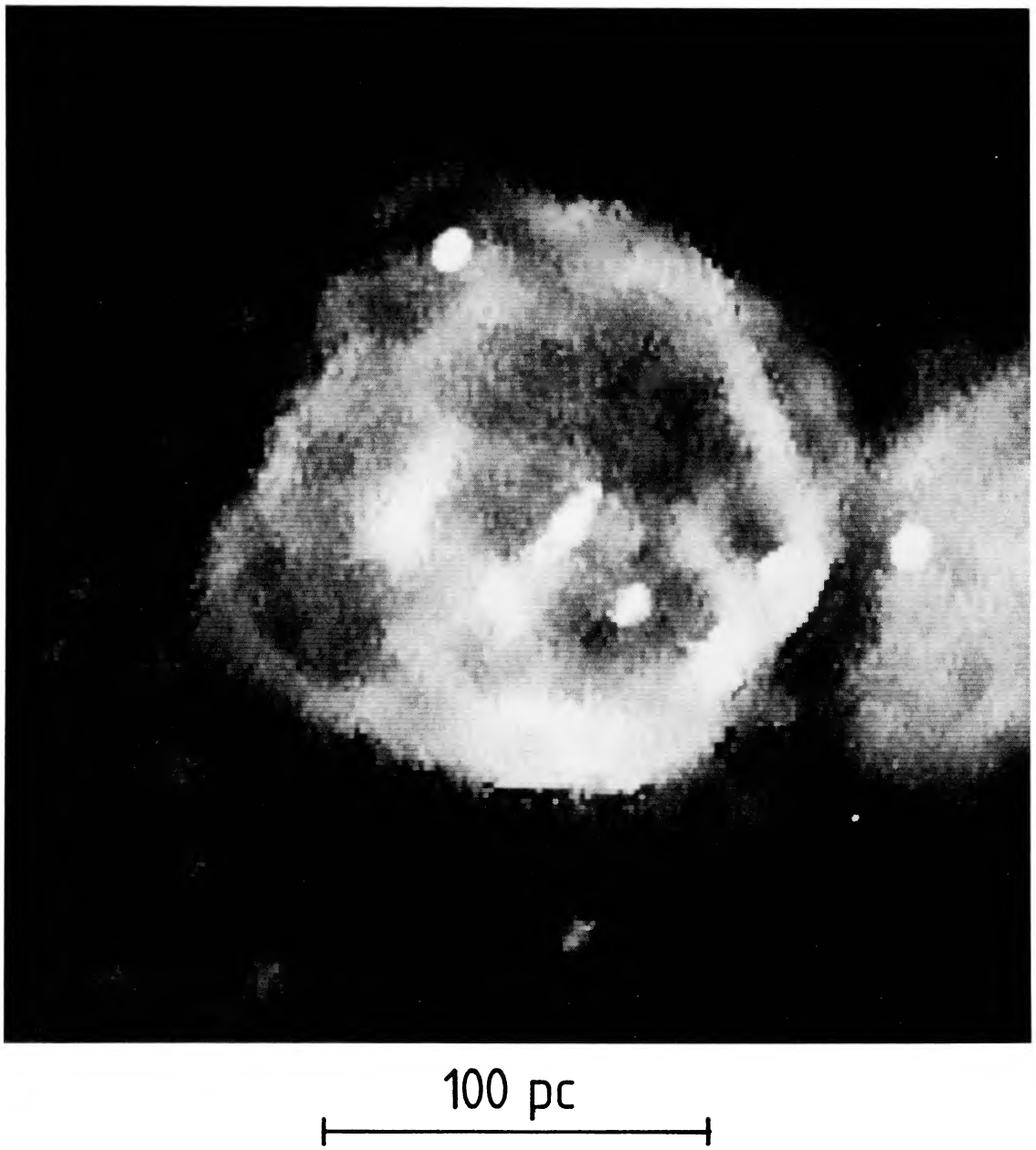

Plate 1. An absolute Hα intensity calibrated image of Hubble III (centre) and Hubble I (right). The image also contains a 5 per cent contribution from [N II].

[*facing page* 494]

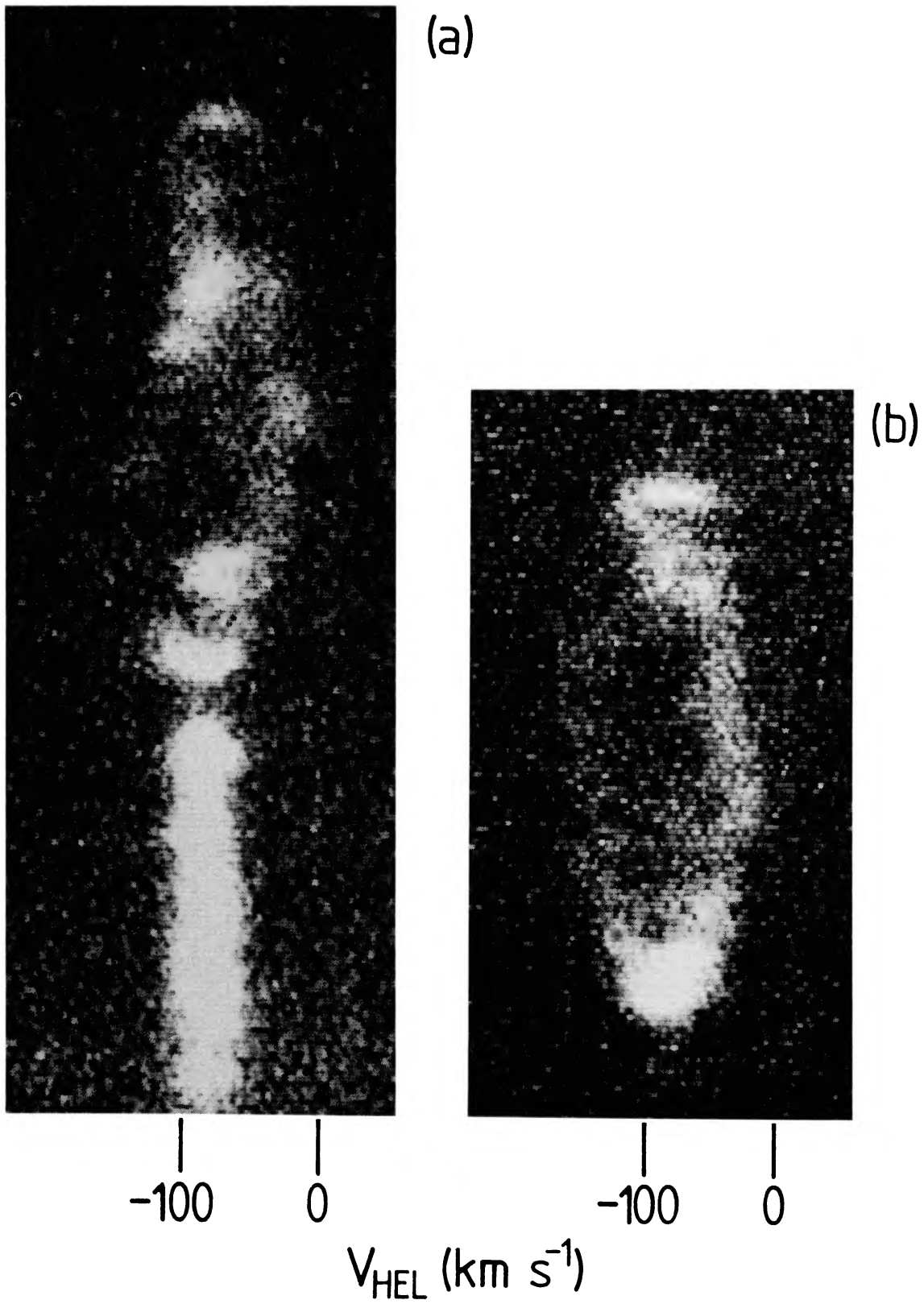

Plate 2. (a) and (b). Grey-scales of parts of the Hα data arrays from slit positions 1 and 2, respectively. High increments are to the top and positive velocities to the right.

both exposures was 3600 s. Grey-scales of the 2D spectra obtained are shown in Plate 2(a) and (b). These nebular emission lines were wavelength-calibrated against Cu/Ar arc lines, using FIGARO routines, to an accuracy of $\pm 1\,\mathrm{km\,s^{-1}}$ in absolute heliocentic velocity. Every six channels along the slit length were coadded to increase the signal-to-noise ratio and the value of V_{Hel} for each velocity component in these profiles was found by determining the least-squares best fit of one or more Gaussians to each profile. This was achieved using the new 2D spectrum analysis program LONGSLIT (Wilkins & Axon, private communication).

The variation in V_{Hel} of the separate Hα velocity components along both slit positions are shown in Fig. 2(a) and (b). Particularly bright components are marked with extra large dots and minor components with empty circles. The dotted lines delineate the presence of spectral features which are not readily apparent in the line profiles when several adjacent slit increments are coadded. These features, however, are clearly visible in Plate 2(a) and (b). The velocity of the surrounding H I is indicated by an arrow.

The velocity fields of Hubble III (see Plate 2 & Fig. 2) show it to be undergoing a remarkably symmetric radial expansion for a nebula of this size (although contraction cannot be ruled out). From these velocity fields, it seems reasonable to conclude that Hubble III closely approximates

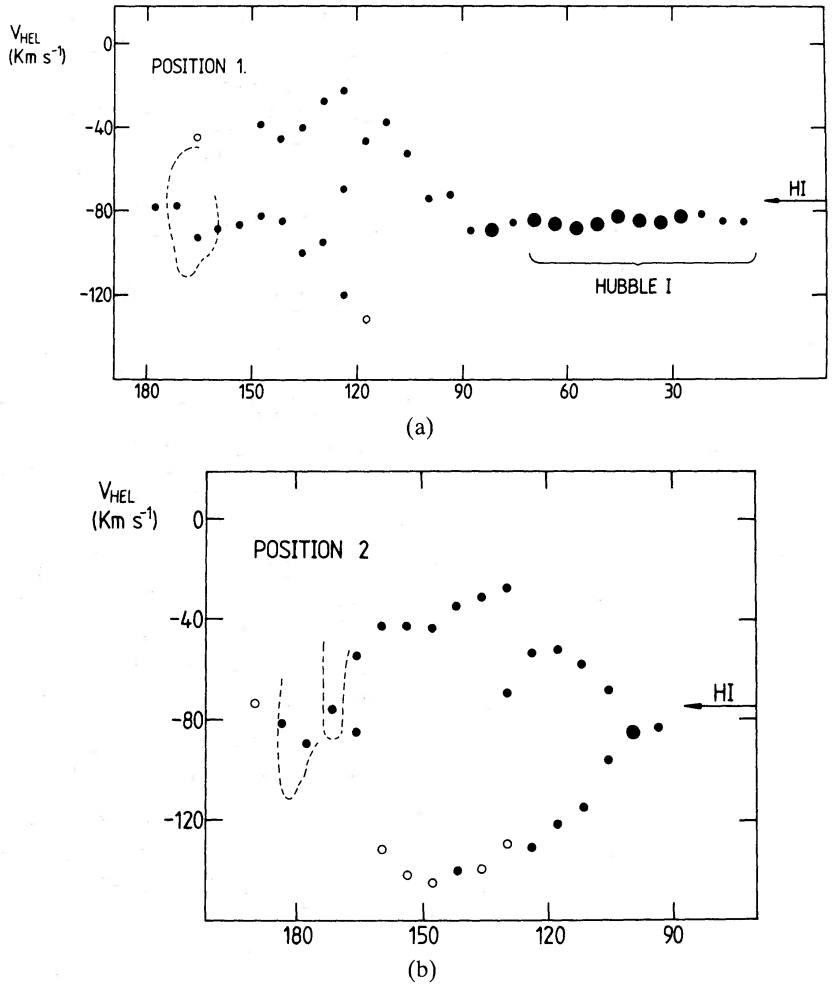

Figure 2. (a, b) The variation of the individual velocity components in the Hα line profiles along slit positions 1 and 2, respectively. The dotted lines indicate features visible in Plate 1(a, b) which are not well seen in the line profiles. The numbers along the bottom indicate increments along the slit (see Fig. 1). The separation of the 30 increment markers corresponds to 42 pc.

to a spherically symmetric bubble 120 pc in diameter expanding at 50 km s^{-1}. In addition, we see on both slits positions what appear to be expanding bubbles at the edge of the main bubble. These again are well-defined radially symmetric bubbles. Comparing the positions along the slits of these small bubbles with Fig. 1 shows that each corresponds to a loop in the filamentary structure at the edge of the ring. Interestingly, the loop covered by slit position 2 has a bright star at its centre. This loop shall be referred to as loop A and the southeastern one as loop B (see Fig. 1). The origin of these features is discussed in Section 3.3.1.

Estimates of the distance to NGC 6822 range from 400 to 620 kpc (see, Mishra 1985, and references therein). Throughout this paper, a value of 500 kpc will be adopted. At this distance, 1 arcsec≡2.4 pc.

3 Discussion

3.1 MORPHOLOGY

Hubble III is morphologically very similar to N70 in the LMC. Both nebulae are highly circular shells comprised of many narrow bright filaments. These filaments suggest a compression of the gas presumably caused by a radiative shock. Estimating the shell thickness is difficult in the case of Hubble III due to its great distance. The shell appears to be made up of several filaments some of whose widths are close to that of the seeing discs of neighbouring stars and which must be very fine. Lower resolution photography (e.g. Hodge 1977) simply shows Hubble III as a simple unstructured ring. The best estimate of the shell thickness has been made from Malin's continuum photograph of NGC 6822 and is ~15 pc. This, however, is a crude estimate and it must be remembered that the shell is, in fact, comprised of several finer filaments. Some of these filaments form loops in the circumference of the ring structure. The two major ones in Hubble III can be seen in Plate 1. Both of these loops were covered by the slit positions. Plate 1 of Blades, Elliott & Meaburn (1980) shows similar loops on the edge of N70. It may be important to note that many of the LMC giant shells have unusual motions around their circumferences, where one would expect a single velocity component. For example, N57 has three separate components over a velocity range of 30 km s^{-1} at its edge (Meaburn & Blades 1980) and similar motions are found at the edges of N70 (Blades *et al.* 1980) and N51 (Meaburn & Terrett 1980). It may be that these observers have detected the effect of small expanding bubbles at the edges of these nebulae, as is seen here in these observations of Hubble III. Lasker (1979) points out that several of the ring nebulae in the LMC also have bright (and possibly hot) stars at or near their edges. These stars may be capable of interacting with their surrounding interstellar material through the action of their stellar winds. Such possibilities are discussed further in Section 3.3.1.

Considerable emission is seen within the ring itself indicating the presence of material along the line-of-sight to the centre of the nebula and suggests a spherical structure. This is in contrast to ring nebulae such as the large H II ring of N44 (Elliott *et al.* 1978) or N59A (Meaburn, Terrett & Blades 1981) in the LMC, which appear more as cylindrical rings rather than as spherical shells.

Gottesman & Weliachew (1977) who have studied the H I content of NGC 6822 have found that Hubble III and many of the other H II regions appear to be located at the edge of, or within a dense ridge of neutral hydrogen to the north–west of the centre of the galaxy. This ridge shows some of the strongest concentration of H I in NGC 6822 and in the vicinity of Hubble III the column density is 40 per cent of its peak value of 2.9×10^{21} cm^{-2}. The symmetry of the velocity field indicates that the 120-pc diameter ring may be completely contained within (or completely outside of) this H I ridge. If this were not the case, either a distorted spherical shell or else a ring structure would have been seen similar to those in N44 and N59A as opposed to the regular shell structure actually observed. The first possibility is quite feasible since Gottesman & Weliachew

(1977) estimate the H I thickness to be at least 200 pc and possibly more. In addition, the symmetry of the expansion implies that the H I must be reasonably homogeneous over at least 120 pc. This compares starkly with the ring nebulae in the LMC whose velocity fields are heavily modified by the clouds of neutral Hydrogen which exist there (McGee & Milton 1966). We find from the observations of Gottesman & Weliachew, that in general, the H I in NGC 6822 is clumpy on the scale of a few hundred parsecs. The neutral hydrogen in the vicinity of Hubble III and I has a mean heliocentric velocity of $-75\,\mathrm{km\,s^{-1}}$ and the systemic velocity of the two nebulae is $-85\,\mathrm{km\,s^{-1}}$ relative to the Sun. Thus, whilst these nebulae are clearly associated with NGC 6822 and not foreground objects, they are not unambiguously associated with the H I ridge.

3.2 STELLAR CONTENT

Unfortunately, no detailed photometry is available for the stars embedded within Hubble III. Hodge (1977) has found 14 stars associated with the nebulosity with $M_V \leq 21$ (corrected for foreground extinction). At a distance of 500 kpc, this corresponds to an absolute magnitude of -2.5. Thus, Hubble III contains the equivalent of 14 ZAMS stars of spectral type B1 or earlier (Panagia 1973). Kayser (1967) describes these stars as being some of the bluest in the whole of NGC 6822. The location of these stars is shown in Fig. 1.

Boggess (1967) obtained *B*- and *V*-band photometry for the stars within all the major H II complexes in NGC 6822. For Hubble III, the four most dominant stars (judged on account of their magnitude, colour and position) were measured and found to have negative values of $B-V$ indicating blue stars. However, these magnitudes are only approximate and are not suitable for determining spectral types. Furthermore, it is not possible to use such photometry to distinguish between O stars of different masses (Massey 1983). However, Boggess does show that the ratio of Lyman continuum photons to visual photons (Q_{LC}/Q_V) obtained from the nebula is close to those obtained by Pottasch (1965) for O4 and O5 stars.

Moffat & Shara (1983) have obtained a spectrum of the star F9 (Kayser 1967) in the centre of Hubble III (see Fig. 1) in order to search for Wolf–Rayet stars in NGC 6822. There is no indication of the 4686 Å bump indicative of Wolf–Rayet stars but comparison of their spectra with the library of Jacoby, Hunter & Christian (1984) does show this to be an early-type star. Exact classification is made difficult by noise level in the spectrum. Incidentally, Moffat & Shara also obtained spectra of the brightest stars/knots in the giant H II regions Hubble X and V but again found no evidence for W–R stars. A more recent search for W–R stars in NGC 6822 carried out by Armandroff & Massey (1985) found 12 W–R candidates but only one of these corresponded to any of the bright emission regions – Hodge 12, which is believed to be a supernova remnant.

Using the total Hα intensity ($I_{H\alpha}$) derived from the calibrated image of Hubble III (Plate 1), we can obtain the total rate of emission of Lyman photons S^* required to radiatively ionize the nebula. This is given (for case B, Osterbrock 1974; Brocklehurst 1971) by

$$S^* = 6.8\times10^{49} I_{H\alpha} D^2\,\mathrm{s^{-1}}$$

where D is the distance to NGC 6822 in pc. For $I_{H\alpha} = 6.6\times10^{-12}\,\mathrm{erg\,s^{-1}\,cm^{-2}}$, we find $S^* = 1.1\times10^{50}\,\mathrm{s^{-1}}$. Panagia (1973) predicts that $S^* = 8.5\times10^{49}$ and $4.2\times10^{49}\,\mathrm{s^{-1}}$ for O4 and O5 stars respectively. Thus, the number of stars ionizing Hubble III correspond to either one or two O4 or three O5 ZAMS. This is in agreement with the number of O4 and O5 stars inferred by Boggess (1967).

3.3 ORIGIN OF HUBBLE III

Any point-like injection of energy into the interstellar medium will produce some form of bubble and it is difficult to determine the nature of the energy source from the morphology of the bubble

alone (Braunsfurth & Feitzinger 1983). In this section, several possible dynamical mechanisms for the creation of Hubble III are examined.

3.1.1 Stellar winds

From the spectroscopic data presented here, we find that Hubble III closely approximates to a spherical bubble expanding at 50 km s^{-1} and with a diameter of 120 pc. The idealistic situation of a stellar wind of power L_w erg s^{-1} from a star located in a uniform cloud of neutral hydrogen of density n_0 atom cm^{-3} has been theoretically described by several workers (e.g. Castor, McCray & Weaver 1975; Dyson 1977; Weaver *et al.* 1977). This stellar wind would produce a spherical bubble of diameter $D(t)$pc, expanding at $V(t)$ km s^{-1} where

$$D(t)=3.5\times10^{-6}V(t)t\,\text{pc} \tag{1}$$

and

$$L_w=9.5\times10^{17}n_0V(t)^5t^2\text{erg s}^{-1} \tag{2}$$

(Meaburn 1980; Weaver *et al.* 1977).
In the case of Hubble III, adopting a value of $n_0=0.8$ cm^{-3} (Gottesman & Weliachew 1977), these predict

$$t=6.9\times10^5\,\text{yr}$$

and

$$L_w=1.1\times10^{38}\,\text{erg s}^{-1}.$$

McCray (1983) gives stellar wind luminosities of up to 2×10^{38} erg s^{-1} for a single O4 I star. The combined winds of several less energetic stars blowing together (e.g. five O4V stars) could easily provide the wind luminosity required to produce the bubble observed.

From the measured Hα intensity and the data available in the literature, it is possible to estimate the mass of the ionized shell. This may be done using two methods; either by evaluating the total mass of ionized gas from the Hα intensity or simply by estimating the number of ionized atoms from the electron density. These two estimates can be derived from the following equations.

$$M_{\text{H II}}=70.2(I_{\text{H}\alpha}D^2xV)^{1/2}M_\odot \tag{3}$$

[assuming case B (Osterbrock 1974; Meaburn 1983) for $T_e\simeq10^4$ K],

$$M_{\text{H II}}=\frac{Vn_e}{40.2}M_\odot \tag{4}$$

where V (pc^3) is the volume of ionized gas, n_e is the electron density ($\langle n_e\rangle_{\text{rms}}=1.7$, Kennicutt 1984), D is the distance to NGC 6822 (pc) and $x\leqq0.1$ for galactic H II regions (Osterbrock & Flather 1959). Taking the shell thickness to be ~15 pc, we obtain H II shell masses of 2.0×10^4 and 2.2×10^4 $M\odot$ from equations (3) and (4), respectively. The close agreement of these values is encouraging. Equations (3) and (4) contain basically the same physics since the value of $\langle n_e\rangle_{\text{rms}}$ from Kennicutt was derived from the Hα flux and recombination theory. Hence the agreement indicates that the Hα calibrations agree. Taking the mean mass, the momentum associated with the ionized shell is thus 2.2×10^{44} g cm s^{-1} and the kinetic energy is 5.3×10^{50} erg. The latter figure is to be compared with the kinetic energy needed from the stellar winds of the central stars ($L_wt=2.4\times10^{51}$ erg) to produce the observed expansion. The difference of a factor of over 2 between this energy requirement and that contained in the ionized gas is not significant. The

discrepancy may be explained if the missing kinetic energy is contained in a neutral gas component surrounding the visible shell. Furthermore, the estimate of the ionized volume is crude.

We thus see that the amount of kinetic energy contained in the ionized shell, the wind luminosity required to account for the observed expansion and ionization requirements of the nebula are all consistent with a model in which several O4V and O5V stars (or their equivalent) are powering the complex. This is in agreement with the estimates of the stellar content described in Section 3.2.

It is now interesting to look at the dynamics of loop A [see Figs 1 & 2(b) and Plate 2(b)]. Here we see a filamentary loop at the centre of which is a bright star and which appears to show a spherically symmetric expansion. By assuming spherical symmetry, we can allow for the fact that the slit position was offset from the centre of this loop. This is done by scaling the observed component of the expansion velocity by the ratio of the full bubble diameter to the length of the slice actually taken across the bubble. This gives a value for the actual velocity of expansion of $V_{exp} \simeq 55\ km\ s^{-1}$ for $D = 30$ pc for this edge bubble. Again applying the stellar wind driven bubble relations given in equations (1) and (2), we predict values of $t = 1.6 \times 10^5$ yr and $L_w = 10^{37}\ erg\ s^{-1}$.

This stellar wind luminosity could easily be provided by a single O5V star (Abbott 1982). Star A is one of the brightest stars in Hubble III and could well be a star of such an early type.

There is observational evidence (e.g. Sancisi 1973; Berkhuijsen 1974) that star formation occurs in spherical shells of gas created by either supernovae, H II regions or wind-driven bubbles. The spherical shock wave produced by the central OB stars may have induced star formation in the surrounding ambient medium. Such stars would be of higher mass than the central stars (Mueller & Arnett 1976; Elmegreen & Lada 1977) due to heating of the ambient medium by the latter and the dependence with temperature of the protostellar mass function (Silk 1977) and would move out with the advancing shock. Such high-mass stars would have strong winds associated with them which would blow small bubbles in the circumference of the main bubble (Fig. 4a). The relative ages of the two bubbles seem consistent with this interpretation, with the age of the edge bubble being ~¼ the estimated lifetime of the main bubble. However, one is then left with the problem of the origin of loop B [which shows a similar velocity field to loop A – see Plate 2(a) and (b)], and the loops on the edge of N70. These features have no apparent sources of kinetic energy at their centres and would have to be produced by another mechanism. It is possible that when pockets of lower density material are encountered by an advancing shock, there is rapid expansion into these regions and blisters are formed on the perimeter of the main bubble (Fig. 4b). Further study of the kinematics of these loops will be necessary before a convincing interpretation of these features can be made. For example, measurements of the Ca II and Na I interstellar absorption-line profiles, in the light of star A, may reveal the approaching component of an expanding bubble. This would confirm that this star is in fact related to the expanding bubble associated with loop A and is not a foreground object.

3.3.2 Supernova action

When a star undergoes a supernova explosion in a uniform medium, it will produce a spherical, collisionally ionized shell. At radio frequencies, this shell will produce considerable non-thermal radiation. As the remnant expands, the non-thermal radio emission will fall off and a neutral shell will result. This shell will then only be visible optically if it is radiatively ionized by, say, other stars in an OB association in which the supernova took place.

From the appearance and kinematics of Hubble III, it is possible that it is a supernova remnant. For example, the fine filaments closely resemble those often observed in SNRs. Using the equations of McKee & Ostriker (1977), it is possible to calculate the maximum size of a supernova

remnant of varying powers in different ambient media. For example, a supernova explosion of energy 3×10^{51} erg in the low-density medium about Hubble III would produce a remnant of maximum size 850 pc. Thus, a remnant 120 pc in diameter would still be far from fossilization.

If Hubble III were indeed such a remnant, it would now be expanding for constant momentum in its snow-plough phase (Chevalier 1974; McKee & Ostriker 1977). Its motion would then be described by the relations

$$E=3.8\times10^{26}n_0^{1.12}V(t)^{4.52}t^{3.12}\text{erg} \tag{5}$$

and

$$D(t)=6.36\times10^{-6}V(t)t\,\text{pc}, \tag{6}$$

where $D(t)$ and $V(t)$ are the diameter (pc) and expansion velocity (km s^{-1}) after time t yr.

For Hubble III these yield

$t=3.8\times10^5$ yr

and

$E=3.6\times10^{51}$ erg.

Thus, a single supernova explosion in the central cluster of stars would be sufficient to generate the kinematics seen. The slightly large estimate of the energy required may be due to uncertainty in the distance to NGC 6822 or possibly due to a small error in V to which E is very sensitive. Alternatively, it might indicate that stellar winds have also been acting on the nebulosity.

Unfortunately, the proposal that Hubble III is an SNR suffers from several drawbacks. In Fig. 3, the values of Log (Hα/[S II]6716 and 6731 Å) are plotted against those of Log (Hα/[N II]6548 and 6584 Å) for Hubble III (Pagel, Edmunds & Smith 1980) and the centre and shell of N70 (Dopita *et al.* 1981). All the intensities are reddening corrected and the underabundance of sulphur and nitrogen in NGC 6822 and the LMC compared with our Galaxy have been taken into account by weighting the intensities by the inverse of the relative abundance of the element producing the line. The LMC is underabundant in N and S by factors of 6 and 2, respectively compared with M42 (Dufour 1975) and NGC 6822 is also underabundant in N by a factor of 6 (Peimbert & Spinrad 1970). The value for S in NGC 6822 is, unfortunately, unknown. However,

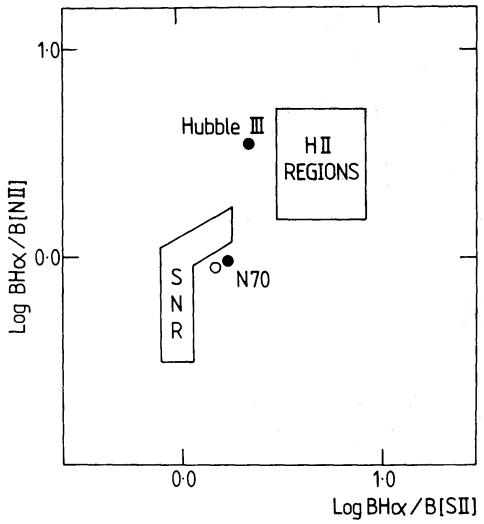

Figure 3. A diagnostic diagram in which the values of Log (BHα/B[N II]) are plotted against Log(BHα/B[S II]) for Hubble III and the core (filled circle) and shell (empty circle) of N70. The regions of the graph occupied by supernova remnants and H II regions are also marked (after Sabbadin *et al.* 1977).

Benvenuti, D'Odorico & Peimbert (1973) have shown that the N/S ratio may be obtained directly from the ratio of [N II] to [S II] lines. Hence, using the line intensities of Pagel *et al.* (1980) we obtain an underabundance of S in NGC 6822 of just under 3.

The regions of the figure normally occupied by various classes of nebulous objects are also shown (Sabbadin, Minello & Bianchini 1977). We see that Hubble III shows more the characteristics of a typical H II region whilst N70 lies close to the region dominated by supernova remnants. However, the corrections for abundance, especially that of S in NGC 6822, are only approximate and hence this diagnosis must be treated with some caution.

Markert & Donahue (1985) have observed NGC 6822 with the *Einstein Observatory* and found only two X-ray sources. X-ray emission would be expected from the hot gas ($T \leqq 10^6$ K) interior of an SNR and which should persist for times $\geqq 10^6$ yr (Cox & Smith 1974). Neither of these correspond to the position of Hubble III [although one does match the position of Hodge 12 (Hodge 1977) which has been classified as a SNR (D'Odorico, Dopita & Benventui 1980) and has $L_x = 10^{37}$ erg]. However, only the most luminous SNRs would be visible since the upper limit of their search corresponds to an X-ray luminosity (L_x) of 5×10^{36} erg (at 500 kpc) and the more typical L_x of an SNR is 10^{35}–10^{36} erg (McCray 1977). The brighter supernova remnants in the LMC would have $L_x \simeq 10^{37}$ erg at this distance. A wind-driven bubble would only have an L_x of 10^{34} erg and this would make a good descriminator between the two dynamical models if greater sensitivity could be achieved.

Finally, the measured temperature of Hubble III is 8800 ± 1000 K (Pagel *et al.* 1980). This is more the value expected in an H II region.

3.3.3 Confined mass-loss bubble (CMLB)

Dopita (1981) has described a type of mass-loss bubble, in which a collapsing H I cloud interacts with the stellar wind from a cluster offset from the mass centre to produce a quasi-steady flow situation. Dopita *et al.* (1981) have applied this model to N70, which is morphologically very similar to Hubble III, and conclude that it is the only dynamical model which fits all the observational facts.

This model is a numerical model and cannot be generally applied. However, certain predictions can be made and tested observationally for Hubble III.

(i) The shape of the nebula is one of the simplest observational tests. The CMLB bubble shape predicted varies from *teardrop to cusp-like* (Dopita 1981; Dopita *et al.* 1981). Furthermore, the mass-loss centre will be displaced from the centre of mass. Fig. 1 shows that Hubble III is a very close approximation to a circle. Also, the centre of that circle is very close to the central star cluster. Any small displacement may be a consequence of the proper motion of the central stars. Weaver *et al.* (1977) have shown that even if the central star(s) move relative to the surrounding medium, the shell will still remain approximately spherical as long as the hot, isobaric layer is within the boundary of the shell. The geometry predicted by the CMLB is not observed.

(ii) The dynamics of the CMLB are quite different to that of an expanding shell. The motions are not radial but transverse in nature and are powered by an oblique stellar wind shock. The predicted velocity field for N70 is shown in fig. 9 of Dopita *et al.* (1981) and is quite unlike the simple expansion seen in Hubble III.

Thus, whilst the CMLB model may seem capable of explaining the origin of N70, it is quite unable to explain the dynamics of Hubble III.

3.3.4 Evolution of an H II region

McKee, Van Buren & Lazare (1984) have described a sequence through which nebulae around massive stars evolve. They begin as wind-blown bubbles and then evolve into amorphous H II

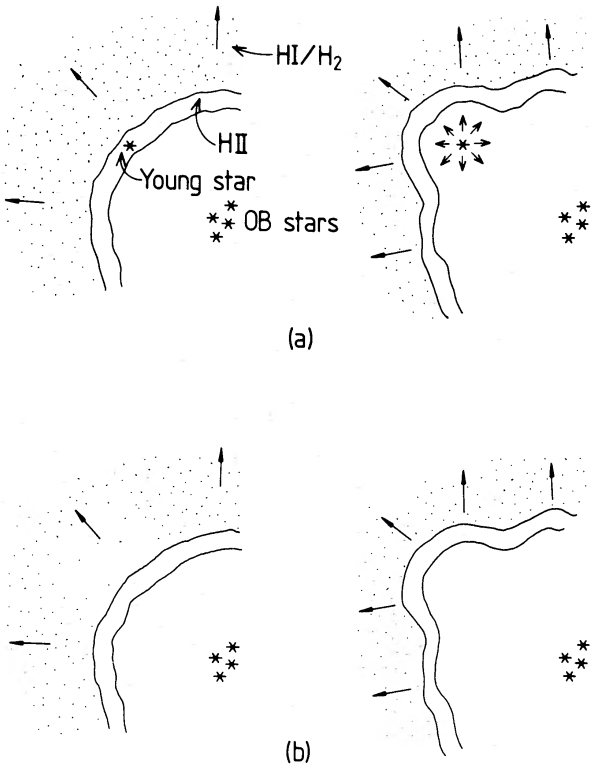

Figure 4. A two-dimensional representation of two possible mechanisms for the formation of edge bubbles. (a) The stellar winds of young high-mass stars produced by the advancing shock can blow out into the surrounding medium. (b) Expansion may occur into pockets of lower density material.

regions, ring-like H II regions, nebulae with stellar ejecta and are finally dominated by the supernova explosion of the central star(s). If such an evolutionary sequence is universal, then the formation of ring nebulae should be a natural stage in the lifecycle of an H II region. Kennicutt (1984) and Braunsfurth & Feitzinger (1983) have also considered the possibility that the ring-like H II regions may be a late stage of evolution of diffuse nebulae. Kennicutt, however, points out that in some galaxies (e.g. IC 1613) the vast majority of H II regions are ring-like and no ring-progenitors are seen.

The gas dynamics around OB associations have been studied numerically by Beltrametti, Tenorio-Tagle & Yorke (1982) and Tenorio-Tagle *et al.* (1982). In brief, they predict that around an evolving OB association a long-lasting, expanding ring-like nebula ($\sim 5\times10^6$ yr) is created as the exciting stars evolve off the main sequence. Gas velocities of up to $40\,\mathrm{km\,s^{-1}}$ are also predicted. This value is an upper limit and does not explain the $50\,\mathrm{km\,s^{-1}}$ motions seen in Hubble III. More importantly, a drop in temperature to ~5000 K in the ionized gas is predicted. This does not agree with the measured temperature of 8800 K. Also the central condensation obtained with some of their models is not seen.

In summary, it would appear that the morphology and kinematics of Hubble III can be best understood in terms of the operation of stellar winds, although the action of supernovae cannot be discounted.

3.4 HUBBLE I

Hubble I is an H II region just NW of Hubble III (see Plate 1). Due to the close proximity of these two objects, it was possible to include both along one slit length (position 1). From the velocity

fields of position 1 it would appear that Hubble I and III are adjacent in space since they both share the same mean heliocentic velocity. Furthermore, the Hα photograph of Boggess (1967) shows that there is an envelope of ionized hydrogen surrounding Hubble I and III and that they are clearly related.

The velocity field over Hubble I shows no evidence for unusual motions. The lack of kinematic structure is surprising since Hubble I contains five blue stars with absolute magnitudes of $\leqq -4.4$ (Boggess 1967). The value of the ratio Q_{LC}/Q_V for Hubble I is consistent with those obtained for O5 and O6 stars (Boggess 1967; Pottash 1965). Furthermore, the position 1 slit passed very close to one of the bright stars at the edge of the nebula (see Fig. 1 and Plate 1) and no kinematic effects due to this star were observed in the neighbouring gas. It is, thus, quite probable that this star is not associated with the nebula and is in fact a foreground object. Images of Hubble I show it to have a fan-shaped structure with a number of bright stars embedded in its base. Considering this morphology and the probable location of Hubble I on/in the H I ridge, one might expect to see a *Champagne* type flow (Tenorio-Tagle 1979). However, no unusual motions were seen (see Fig. 2a).

Hippelein (1986) has found a correlation between Hα luminosities and Hα velocity dispersions in giant H II complexes. In order to test this relationship, the line profiles across the whole of Hubble I (position 1, increments 1–72) were coadded and a single Gaussian was fitted by least squares to the resulting near-Gaussian profile. A σ_{obs} of $17.9\pm0.1\,km\,s^{-1}$ was found. This was corrected for instrumental broadening ($\alpha_{inst}\simeq 10\,km\,s^{-1}$), broadening due to the fine structure of the hydrogen line and thermal broadening (adopting $T_e=12\,000\pm1200$, Pagel *et al.* 1980) yielding a velocity dispersion of $\sigma=10.4\pm0.5\,km\,s^{-1}$. Using the H$\alpha$ luminosity of Boggess (1967) of $1.1\times10^{38}\,erg\,s^{-1}$, the luminosity–turbulence relation of Hippelein predicts a velocity dispersion of $\sigma=10.2\pm1.7\,km\,s^{-1}$ which agrees well with the observed value.

It is also interesting to note that the uncorrected velocity dispersion of small regions of Hubble I (coadding six slit increments) vary only from 17 to $20\,km\,s^{-1}$, with a mean of $18\pm1\,km\,s^{-1}$. This indicated that the full velocity dispersion is present in small regions of the nebula and is not a consequence of the coaddition of the velocity profiles from many regions with differing velocity dispersions. Nor is it due to low spatial resolution observation of organized motions on the scale of the size of the nebula. Such motions have been seen to affect the velocity dispersion in many other H II complexes (see, e.g. Meaburn 1984; Clayton 1986; Clayton & Meaburn 1987) and their effects should be considered when using Hα luminosity/velocity dispersion relationships to determine extragalactic distances.

Acknowledgments

The author would like to thank J. Meaburn for generously donating Manchester Echelle commissioning time for this project and for his advice and assistance and that of the staff of the INT in 1986 June when these observations were made. I am also grateful to the SERC for my research studentship and W. V. Garner for printing the photographs so well.

References

Abbott, D. C., 1982. *Astrophys. J.*, **263,** 723.
Armandroff, T. E. & Massey, P., 1985. *Astrophys. J.*, **291,** 685.
Beltrametti, M., Tenorio-Tagle, G. & Yorke, H. W., 1982. *Astr. Astrophys.*, **112,** 1.
Benvenuti, P., D'Odorico, S. & Peimbert, M., 1973. *Astr. Astrophys.*, **28,** 447.
Berkhuijsen, E. M., 1974. *Astr. Astrophys.*, **35,** 429.
Blades, J. C., Elliott, K. H. & Meaburn, J., 1980. *Mon. Not. R. astr. Soc.*, **192,** 101.
Boggess, N., 1967. *PhD thesis,* University of Michigan.

Boksenberg, A. & Burgess, D. E. 1973. *Proc. Symp. TV Sensors,* p. 21, University of British Columbia, Vancouver.
Braunsfurth, E. & Feitzinger, J. V., 1983. *Astr. Astrophys.,* **127,** 113.
Brocklehurst, M., 1971. *Mon. Not. R. astr. Soc.,* **153,** 471.
Castor, J., McCray, R. & Weaver, R., 1975. *Astrophys. J.,* **200,** L107.
Chevalier, R. A., 1974. *Astrophys. J.,* **188,** 501.
Clayton, C. A., 1986. *Mon. Not. R. astr. Soc.,* **219,** 895.
Clayton, C. A. & Meaburn, J., 1987. *The Observatory,* in press.
Cox, D. P. & Smith, B. W., 1974. *Astrophys. J.,* **189,** L105.
D'Odorico, S., Dopita, M. A. & Benvenuti, P., 1980. *Astrophys. J. Suppl.,* **40,** 67.
Dopita, M. A., 1981. *Astrophys. J.,* **246,** 65.
Dopita, M. A., Ford, V. L., McGregor, P. J., Mathewson, D. S. & Wilson, I. R., 1981. *Astrophys. J.,* **250,** 103.
Dufour, R. J., 1975. *Astrophys. J.,* **195,** 315.
Dyson, J. E., 1977. *Astr. Astrophys.,* **59,** 161.
Elliott, K. H., Goudis, C., Meaburn, J. & Pilkington, J., 1978. *Astrophys. Space Sci.,* **55,** 475.
Elmegreen, B. G. & Lada, C. J., 1977. *Astrophys. J.,* **214,** 725.
Gottesman, S. T. & Weliachew, L., 1977. *Astr. Astrophys.,* **61,** 523.
Hippelein, H. H., 1986. *Astr. Astrophys.,* **160,** 374.
Hodge, P. W., 1977. *Astrophys. J. Suppl.,* **33,** 69.
Hubble, E., 1925. *Astrophys. J.,* **62,** 409.
Jacoby, G. H., Hunter, D. A. & Christian, C. A., 1984. *Astrophys. J. Suppl.,* **56,** 257.
Kayser, S. E., 1967. *Astr. J.,* **72,** 134.
Kennicutt, R. C., 1984. *Astrophys. J.,* **287,** 116.
Lasker, B. M., 1979. *Publs astr. Soc. Pacif.,* **91,** 153.
Lee, J. S., 1981. *Comp. Graph. Image Processing,* **15,** 380.
McCray, R., 1977. In: *Topics in Interstellar matter,* p. 35, ed. van Woeden, H., Reidel, Dordrecht, Holland.
McCray, R., 1983. In: *Highlights of Astronomy,* Vol. 6, ed. West, R. M., Reidel, Dordrecht, Holland.
McGee, R. X. & Milton, J. A., 1966. *Aust. J. Phys.,* **19,** 345.
McKee, C. F. & Ostriker, J. P., 1977. *Astrophys. J.,* **218,** 148.
McKee, C. F., Van Buren, D. & Lazareff, B., 1984. *Astrophys. J.,* **278,** L115.
Malin, D. & Murdin, P., 1984. *Colours of the Stars,* p. 170, Cambridge University Press.
Markert, T. H. & Donahue, M. E., 1985. *Astrophys. J.,* **297,** 564.
Massey, P., 1983. *Publs astr. Soc. Pacif.,* **97,** 5.
Meaburn, J., 1980. *Mon. Not. R. astr. Soc.,* **192,** 365.
Meaburn, J., 1981. In: *Investigating the Universe,* p. 61, ed. Kahn, F. D., Reidel, Dordrecht, Holland.
Meaburn, J., 1983. *Astr. Astrophys,* **122,** 111.
Meaburn, J., 1984. *Mon. Not. R. astr. Soc.,* **211,** 521.
Meaburn, J. & Blades, J. C., 1980. *Mon. Not. R. astr. Soc.,* **190,** 403.
Meaburn, J. & Terrett, D. L., 1980. *Astr. Astrophys.,* **89,** 126.
Meaburn, J., Terrett, D. L. & Blades, J. C., 1981. *Mon. Not. R. astr. Soc.,* **197,** 19.
Meaburn, J., Blundell, B., Carling, R., Gregory, D. F., Keir, D. & Wynne, C., 1984. *Mon. Not. R. astr. Soc.,* **210,** 463.
Mishra, R., 1985. *Mon. Not. R. astr. Soc.,* **221,** 163.
Moffat, A. F. J. & Shara, M. M., 1983. *Astrophys. J.,* **273,** 544.
Mueller, M. W. & Arnett, W. D., 1976. *Astrophys. J.,* **210,** 670.
Osterbrock, D. E., 1974. *Astrophysics of Gaseous Nebulae,* Freeman and Co., San Francisco.
Osterbrock, D. E. & Flather, E. M., 1959. *Astrophys. J.,* **129,** 235.
Pagel, B. E. J., Edmunds, M. G. & Smith, G., 1980. *Mon. Not. R. astr. Soc.,* **193,** 219.
Panagia, N., 1973. *Astr. J.,* **78,** 929.
Peimbert, M. & Spinrad, H., 1970. *Astr. Astrophys.,* **7,** 311.
Pottasch, S. R., 1965. *Vistas Astr.,* **6,** 149.
Sabbadin, F., Minello, S. & Bianchini, A., 1977. *Astr. Astrophys.,* **60,** 147.
Sancisi, R., 1973. In: *Proc IAU Symp. No. 60, Galactic Radio Astronomy,* p. 115, eds Kerr, F. J. & Simonson III, S. C., Reidel, Dordrecht, Holland.
Seaton, M. J., 1979. *Mon. Not. R. astr. Soc.,* **187,** 73P.
Silk, J., 1977. *Astrophys. J.,* **214,** 718.
Tenorio-Tagle, G., 1979. *Astr. Astrophys.,* **71,** 59.
Tenorio-Tagle, G., Beltrametti, M., Bodenheimer, P. & Yorke, H. W., 1982. *Astr. Astrophys.,* **112,** 104.
Weaver, R., McCray, R., Castor, J., Shapiro, P. & Moore, R., 1977. *Astrophys. J.,* **218,** 377.